



Influence of Geotechnical Parameters and In-Situ Stresses on Strainburst Potential

N. Ramirez and A. Delonca^(✉)

Department of Metallurgical Engineering and Materials, Universidad Técnica Federico Santa María, Santiago, Chile
adeline.delonca@usm.cl

Abstract. As a result of the intense exploitation of mineral resources on the surface, mining excavations must migrate to deeper environments. At greater depths, in-situ stresses increase along with the probability of rockburst occurrence. Different authors have studied this phenomenon in depth, however, the influence of the variability of environmental parameters on rockburst potential has not been studied in detail. This paper proposes to respond to this limit. More than 300 numerical models have been ran using Rs3 software to perform a sensitivity analysis of the main geomechanical parameters of the environment such as UCS, GSI, rock density and the elastic parameters (Young and Poisson's modulus). Moreover, various depths have been considered to vary the in-situ stress. The Damage Initiation Spalling Limit (DISL) approach proposed by Diederichs (2007) has been considered to simulate the brittle failure of the rock mass and estimate the depth of failure around the excavation in all simulations. This work highlights the influence of the uniaxial compressive strength (UCS) and the in-situ stresses over the rest of the parameters. The elastic parameters of the rock mass do not influence excavation instability. Moreover, the GSI has no influence in our study. This can be explained knowing that small GSI values have been considered, according to "El teniente" mine, and therefore rockburst might not occur. To better understand the GSI influence on rockburst potential, its influence has been compared with Hoek & Brown failure criterion. Based on this work, a series of recommendation when simulating deep excavation is provided.

Keywords: Rockburst · Deep tunnel · Numerical modelling · UCS influence

1 Introduction

Various unwanted phenomena can occur in underground mining, and rockburst are one of these. They can be defined as a dynamic phenomenon of brittle failure of the rock mass that manifests itself in the sudden and often violent ejection of a large volume of rock that detaches from the advancing front or from the contour of an underground excavation [1]. This rock ejection can cause severe damage to the excavation as well as to machines and people working on the ground. In the last decades, techniques based on numerical models have shown their potential to investigate in depth the phenomenon

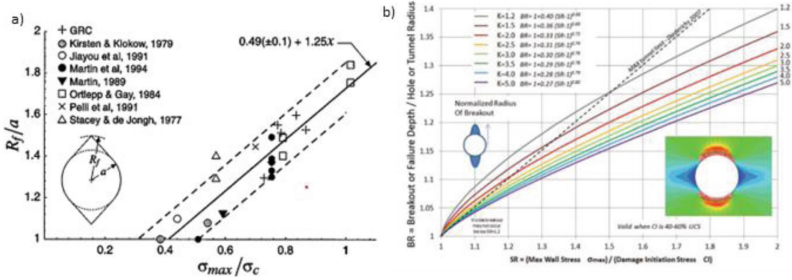


Fig. 1. (a) Martín [2] and (b) Diederichs [4] method to determine depth of failure

of rockburst and its triggering mechanisms. There are different authors that have developed empirical methods based on historical cases [2, 3] and analytical methods using numerical modeling [4] to relate and determine the depth of failure in deep excavations. On the other hand, different authors have studied this phenomenon (many of them using numerical modeling) with respect to determining its occurrence’s mechanism, how to assess its magnitude [2, 3, 5] and how to prevent them [6]. However, the influence of the variability of the geomechanical parameters of the rock mass has not been studied in depth while it can have a strong impact on the rockburst level assessment. In this paper, numerical modeling is used to study the rockburst phenomenon in deep excavation. More specifically a sensitivity analysis of different study parameters is performed to see the influence of their variability on the depth of failure of a rockburst.

1.1 Rockburst’s Depth of Failure Assessment

To date, it is complex to predict the moment, location, and magnitude of a rockburst. However, it is possible to get closer to these three components considering some empirical, analytical and/or numerical methods that have been developed by different authors. Martin et al. [2] proposed an empirical graph to determine the depth of failure (Fig. 1a) in an unstable excavation considering about twenty-three historical cases of brittle failure with spalling. They determined that when σ_{max}/σ_c is greater than 0.4, instability occurs. Diederichs [4] proposes a depth of failure prediction graph that is more rigorous (Fig. 1b), based on numerical modeling analysis using the Damage Initiation Spalling Limit (DISL) approach [7]. The DISL approach was developed to simulate the brittle failure of the rock mass in conventional engineering software. It is based on the generalized failure criterion of Hoek & Brown [8] modifying the peak and residual resistance parameters as shown in Table 1. The author was able to estimate the maximum depth of failure for a deep circular tunnel for each “K” value (ratio between the two principal stresses).

2 Methodology

378 numerical models were run using the RS3 software to simulate the opening of a deep underground tunnel. The basic model consists in a box of 30 m by 30 m, with a tunnel in the center of 5 m of diameter. An elastoplastic model is assumed for the rock mass

Table 1. Peak and Residual parameter proposed by Diederichs [4]

Peak		Residual	
Parameter	Value	Parameter	Value
a_p	0.25	a_r	0.75
s_p	$(CI/UCS)^{\frac{1}{a_p}}$	s_r	0.001
m_p	$s_p \times \frac{UCS}{T}$	m_r	6-12

surrounding the tunnel. The brittle rock failure behavior is define considering the DISL approach. The base model (or first model) considers an unstable excavation presenting spalling (great depth, good quality of rock mass and $m_i = 25$) and assesses the rockburst potential considering the depth of failure around the excavation, and the failure angle and width. The advancing front is assessed when half tunnel has been built. To assess the rockburst potential, the yielded elements are observed. When there is 100% of yielded elements, it is assumed that the zone is failed. Variability in the models is integrated based on first unstable model by modifying various parameters according to Table 2. The models consider an Andesite rock, as it presents the typical high strength needed to the rockburst occurrence.

A different model is run each time a parameter is modified. The base model includes the average values of each parameter at a depth of 1500 m, when all models have been run, the depth of the excavation is increased by 500 m. It is well known that burst should not occur for GSI values less than 65–70 [7], however, there are cases of smaller GSI rock masses in “El Teniente” mine (where rockburst occur) and their values are included in this work. To assess the influence of each parameter, a sensitivity analysis is carried out considering an increase factor. This increase factor is defined as the relationship

Table 2. Variation range of geomechanical parameters

Parameters	Range	Interval	Number of models	Source
UCS (MPa)	120 – 270	25	90	Gonzalez de Vallejo (2002)
E (Gpa)	30 – 50	4000	42	
ν	0.20 – 0.30	0.02	42	
Rock density (ton/m^3)	2.50 – 2.85	0.05	64	Vergara (2006)
GSI	55 – 85	5	98	
Diameter (m)	5 – 10	5	42	
Depth (m)	1500 – 4000	500	6 loops	

between the measured depth of failure (or other rockburst potential indicator) and the initial value for the initial model.

3 Results

Figure 2 presents the influence of the UCS based on the graph made by Martín et al. [2]. This includes the failure envelopes presented previously, and the depth of failure measurements normalized by the radius of the excavation “a”, when the UCS parameter is varied. It allows us to validate that these results coincide with the literature reviewed and generates confidence to continue running the remaining models. Table 3 shows the measured depth of failure (D_f) obtained at 1,500 m of depth when the geomechanical and elastic parameters value is varied as defined Table 2. It highlights the uniaxial compression strength (UCS) as the parameter that presents the greatest variation between the maximum and minimum measured depth of failure. When the UCS’s magnitude is doubled, the depth of failure is reduced to 30% of the initial measurement. As the GSI increases, the depth of failure is always the same measure and when the value of the rock density is increased up to 20%, the depth of failure also increases by the same percentage. Moreover, the influence of the elastic parameters analyzed shows minimal influence.

Figure 3 shows the increase factor for each geomechanical parameter (UCS, GSI and rock density). Moreover, the figure proposes to approximate a trend line. The UCS and the depth of the excavation are the parameters that has more influence on variation of the measured depth of failure.

During the sensitivity analysis it was observed that the depth of the excavation (therefore the in-situ stresses) has considerably influenced the severity of a rockburst. The results shown in Fig. 3c, when the depth is doubled from 1500 to 3000 m, on average, the depth of failure measurement increases up to 230%. This paper also analyzes the measurements of the unstable advancing front when half excavation has been built and

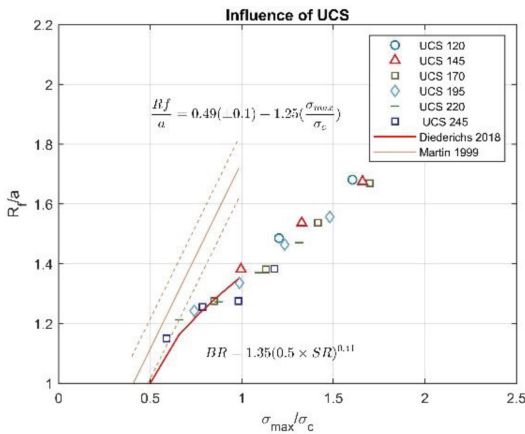


Fig. 2. Influence of uniaxial compressive strength (UCS)

Table 3. Measurements obtained from the variation of geomechanical and elastic parameters

Geomechanical parameters					Elastic Parameters				
UCS (Mpa)	D _f (m)	GSI	D _f (m)	Rock density (ton/m ³)	D _f (m)	Poisson's Module	D _f (m)	Young's Module (Gpa)	D _f (m)
120	1.2	55	0.6	2.50	0.5	0.20	0.6	30	0.6
145	1.0	60	0.6	2.55	0.5	0.22	0.6	34	0.6
170	0.7	65	0.6	2.60	0.6	0.24	0.6	38	0.6
195	0.6	70	0.6	2.65	0.6	0.26	0.6	42	0.6
220	0.5	75	0.6	2.70	0.6	0.28	0.6	46	0.6
245	0.4	80	0.6	2.75	0.6	0.30	0.6	50	0.6

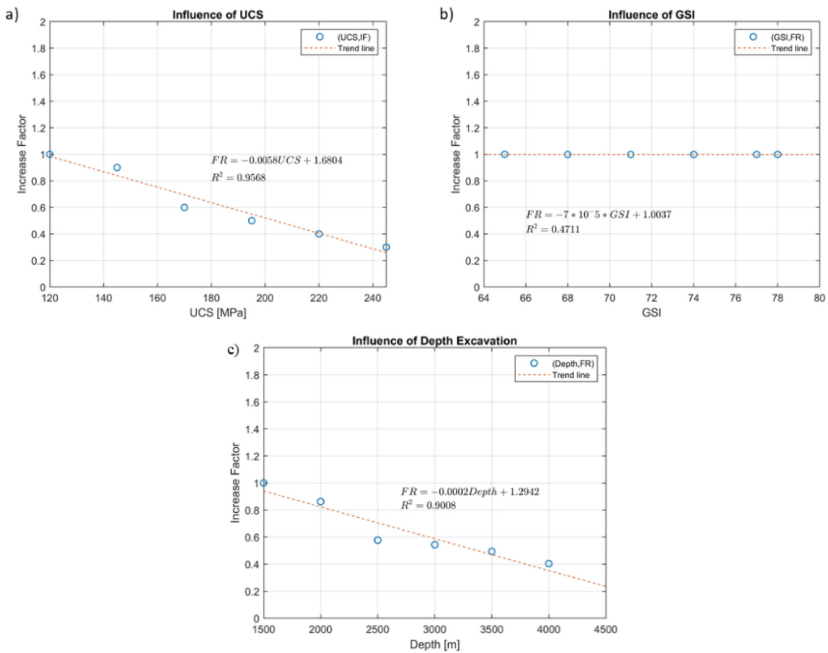


Fig. 3. Influence of geomechanical parameters: (a) UCS; (b) GSI; (c) Excavation Depth

the scale effect is slightly studied by running the same models considering doubled diameter. The results are shown in Table 4 and it is observed that these measurements behave similarly in comparison with previously parameters studied (biggest influence of UCS). Considering D5 and D10 like 5- and 10-m diameter and the comparison between both depth of failure normalized by the radius of the excavation and show us no increase in D_f/a factor when diameter of the excavation is increased.

Table 4. Influence of UCS and GSI on the advancing front (Red) and influence of diameter

UCS (MPa)	Advancing front (m)	GSI	Advancing front (m)	Diameter (m)	D _f (m)	D _f /a
120	1.6	55	1.1	2	0.24	0.24
145	1.3	60	1.1	4.5	0.54	0.24
170	1.2	65	1.1	5	0.58	0.23
195	1.1	70	1.1	6	0.71	0.23
220	0.8	75	1.1	7	0.76	0.22
245	0.0	80	1.1	10	1.24	0.24

4 Discussion

The results shown previously are consistent with the literature reviewed, when σ_{max}/UCS is greater than 0.4, instability occurs. As expected, the geomechanical parameters of the environment influence more than elastic parameters. The non-influence of the GSI was to be expected for quality of rock masses less than $GSI = 65$. Considering that it is well assumed by the community that rockburst occur in good to very good rock masses quality [7]. This section attempts to respond GSI behavior for values less than 65–70 where bursting does not occur, but El teniente mine has rock masses with that quality and less. There are other more important parameters such as strain rate [7], however, the approach of this study is to determine the influence of the input parameters to simulate underground excavations. The influence of the increase of the GSI is studied in new models considering the Hoek & Brown criterion [8], which directly includes the blocosity of the rock mass. Figure 4 shows the wide difference between both approaches and is notable that models that uses the Hoek & Brown criterion allows a considerable influence of the GSI parameter to be highlighted. This can be explained since the DISL approach used throughout this work does not directly include the GSI in the calculation of the parameters. After these new models, when GSI is varied considering DISL approach, the difference between the maximum and minimum depth of failure measurement is just 5%, while using Hoek & Brown criteria, the difference increases up to 68%.

5 Conclusions and Recommendations

Throughout this work, the “DISL” method proposed by Diederichs (2007) was used, which represented a solid and robust tool specially designed for the simulation of brittle failure behavior in conventional engineering software such a Rs3. The depth of failure is considered a good indicator to measure the severity of a rockburst. In this project, the results concur with literature reviewed as to the instability of deep excavation. Regarding in-situ stresses, throughout this work they have shown to categorically influence on the severity of a rockburst even more than expected. When the depth at which the excavation is simulated is doubled from 1,500 to 3,000 m, the depth of failure increases up to 230%, evidencing a clear and considerable influence similar to that of the “ucs”, but no greater.

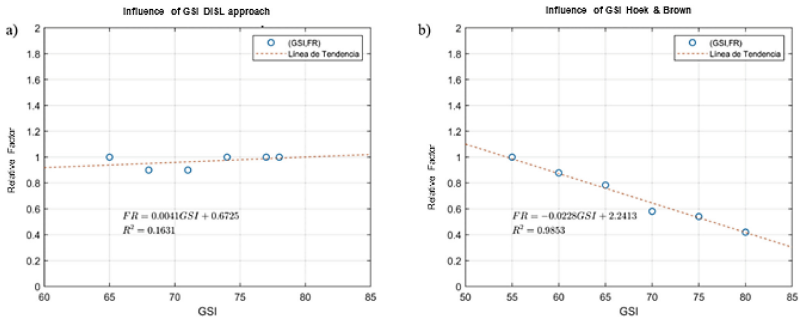


Fig. 4. Influence of the GSI comparing the DISL approach (a) and Hoek & Brown criteria (b)

When the magnitude of the “ucs” is doubled the depth of failure decrease up to 30% or one third of initial measurement and when the rock density is increased by 10%, the depth of failure increases in the same proportion. The scale effect is studied by varying the diameter of the excavation, this produces an increase in the depth of failure, however, “ D_f/a ” ratio varies slightly less than 10%. When comparing the influence of the “gsi” with different approaches, it shows us an increase close to 60% in the variation of the depth of failure. There is a great difference in the depth of failure measurements between the different approaches used for blocky rock masses that is beyond to scope of this project and we propose to consider the fracturing of the rock mass in its definition. We recommend focusing in collecting reliable information of the geomechanical parameters of the rock mass to simulate underground openings including in situ stress. Also, we recommend an in-depth study in terms of the GSI influence with different approaches including scale effect to see more about that anomaly and to simulate very deep mining and its support methods and carry out studies focused on in-situ stress. These areas are a good topic to develop in future research. Our industry needs to build safe deep excavations, and this work recommends investigating more and more about underground mining with modelling simulation that is a very useful tool to achieving that goal.

Acknowledgements. This research has been supported by the National Agency for Research and Development of Chile (ANID) with grant FONDECYT 11200156.

References

1. Zhang, W.: A rockburst intensity criterion based on the Geological Strength Index. *Bulletin of Engineering Geology and the Environment* (79), (2020).
2. Martín, C. D., Kaiser, P. K., McCreath, D. R.: Hoek-Brown parameters for predicting the depth of failure around tunnels. *Canadian Geotechnical Journal* 1(36), 136–151 (1999).
3. Mitri, H. S., Tang, B., Simon, R.: FE modelling of mining-induced energy release and storage rates, p. 8 (1999).
4. Diederichs, M.: Early assessment of dynamic rupture hazard for rockburst risk management in deep tunnel projects. *Journal of the Southern African Institute of Mining and Metallurgy* (118), 193–204 (2018).

5. Kaiser, P. K.: Canadian Rockburst Support Handbook. Geomechanics Research Centre, (1996).
6. Zhang, H., Sun, J., Yang, J.: The Spatiotemporal distribution law of microseismic event and rockburst characteristics of the deeply buried tunnel group. *Energies* 1(11), (2018).
7. Diederichs, M. S.: Mechanistic interpretation and practical application of damage and spalling prediction criteria for deep tunneling. *Canadian Geotechnical Journal* 9(44), 1082–1116 (2007).
8. Hoek, E., Carranza, C., Corkum, C.: Hoek-brown failure criterion 2002 - edition. *Proceedings of NARMSTac*, 1(1), 267–273, (2002).

Open Access This chapter is licensed under the terms of the Creative Commons Attribution-NonCommercial 4.0 International License (<http://creativecommons.org/licenses/by-nc/4.0/>), which permits any noncommercial use, sharing, adaptation, distribution and reproduction in any medium or format, as long as you give appropriate credit to the original author(s) and the source, provide a link to the Creative Commons license and indicate if changes were made.

The images or other third party material in this chapter are included in the chapter's Creative Commons license, unless indicated otherwise in a credit line to the material. If material is not included in the chapter's Creative Commons license and your intended use is not permitted by statutory regulation or exceeds the permitted use, you will need to obtain permission directly from the copyright holder.

